

DMSO-based photonic crystal fiber sensor with enhanced sensitivity

Ali H. Abdulhadi¹, Sun-jie Qiu², and A. Hadi Al-Janabi^{1*}

¹*Institute of Laser for Postgraduate Studies, University of Baghdad, Iraq*

²*College of Engineering and Applied Sciences, Nanjing University, Nanjing 210093, China*

*Corresponding author: hadi.janabi@ilps.uobaghdad.edu.iq

Received August 12, 2013; accepted December 19, 2013; posted online January 27, 2014

We construct a dimethylsulfoxide (DMSO)-based photonic crystal fiber (PCF) temperature sensor with enhanced sensitivity. A solid-core PCF with large mode area is employed to supply the in-line Mach-Zehnder interference between the fundamental and cladding modes. Thus, temperature sensing can be realized because of the shift of interference spectrum at different temperatures. The DMSO solvent is infiltrated between the main sensor and a silica tube to increase the temperature sensitivity of the sensor. The obtained sensitivity (0.315 nm/°C) is one or two orders of magnitude higher than that of previously published results. The proposed sensor is adapted for high-temperature sensing.

OCIS codes: 060.0060, 060.2370, 060.5295, 060.2430.

doi: 10.3788/COL201412.020603.

In-line fiber modal interferometer is widely used in various sensing applications. Among them, temperature sensing by using a conventional optical fiber is a very promising example^[1–3]. Photonic crystal fiber (PCF)-based in-line modal interferometer, which has unique guiding mechanisms and modal properties, has shown many advantages in these applications^[4,5]. Different PCF sensors based on modal interferometers are designed and constructed to detect temperature, strain, refractive index, and others^[6,7]. High-sensitivity temperature sensors based on PCF are still difficult to achieve because of the low thermo-optic and thermal expansion coefficient of fused silica (PCF material)^[8]. A typical PCF-based modal interferometer is obtained by sandwiching a PCF between two single mode fibers (SMFs). Although different fabrication techniques, such as long period grating, micro hole-collapsing, and tapering^[9–11], have been attempted, these structures normally provide low temperature sensitivity. One way to increase the PCF temperature sensitivity is to infiltrate liquids with high thermo-optic and thermal expansion coefficients into the holes of PCF^[12]. However, the infiltration of liquids inside the holes of PCF remains a challenge because of splicing difficulty and evaporation effects of solvents during splicing. Nevertheless, long lengths of expensive polarization maintaining PCF have been used to enhance temperature sensitivity^[13]. To the best of our knowledge, all liquids that infiltrate PCF temperature sensor are limited to temperatures below 100 °C. Recently, Zhang *et al.*^[14] proposed a Fabry-Perot interferometer by using polarization-maintaining photonic crystal fiber for high temperature sensing with maximum obtained sensitivity of 13.8 pm/°C. Therefore, developing a cost effective PCF-based sensor with operation temperatures over 100 °C with high sensitivity is of great importance.

In this letter, we construct a PCF temperature sensor based on external infiltration of high thermo-optic coefficient solvent, that is, dimethylsulfoxide (DMSO). DMSO is a safe solvent for both synthesis and formula-

tion applications. This solvent has been used in medical and chemical applications that could be found in several nuclear magnetic resonance spectrometers and micro-electronic devices^[15]. High boiling point (189 °C), low evaporation effects at low temperature range, and low toxicity contribute to the use of the DMSO in the experiment. Thus, a new PCF sensor with high temperature sensitivity is expected. This compact, rigid, responsive, and highly sensitive device can be incorporated in alarm systems and can withstand harsh environments.

In our experiment, a 2.3-cm-long large mode area (LMA-8, NKT photonics, Denmark) PCF is used. The PCF has an 8.4- μm core diameter and voids with an average diameter of 2.17 μm and an average separation of 5.3 μm between voids (see Fig. 1(a)). This kind of fiber has been used to build the in-fiber modal interferometer^[11,12]. The process to build the interferometer in the PCF by using a fusion splicer is simple. A manual mode of a standard fusion splicer has been selected because no special fusion splicer is available. Optimal parameters for splicing have been chosen manually. The separation of fusion splicer arc electrode is controlled through the screen display of the fusion splicer. The display indicates the exact distance. Thus, fusion splicing can be carried out reliably by adjusting the electrode tip. In our experiment, LMA-8 PCF is spliced in both sides with two conventional single mode fibers (SMF-28, Corning, USA). The modal interference comprises a sandwich configuration of SMF-PCF-SMF. The similar diameter of LMA-8 and SMF-28 makes the light easier to be coupled in the splicing point^[16]. To excite the fundamental and cladding modes, a full collapse of PCF air holes is achieved during fusion splicing. The length of the collapsed region is fully controlled by adjusting the fusion splicer power and the fusion time. The collapse of PCF holes creates the interferometer, and the length of PCF affects the fringe visibility of the sensor. The collapsed length of PCF was $\sim 340 \mu\text{m}$. Figure 1(b) shows the microscopic image of the PCF-SMF splicing area.

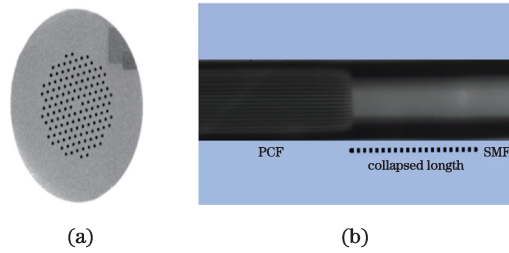


Fig. 1. (Color online) (a) Cross section of a PCF under the scanning electron microscope; (b) microscopic image of the PCF-SMF splicing area showing the collapsed length.

Before the fusion splicing process, the coating of LMA-8 PCF was stripped and split by using a high-quality fiber cleaver to provide access to the evanescent field of the PCF. After the fusion splicing process, a silica tube with 1-mm diameter and $\sim 350\text{-}\mu\text{m}$ thickness (fabricated in Jiangsu, China) was used in the experiment to confine the DMSO outside the PCF region. The tube length was almost the same as the PCF length. Subsequently, DMSO was infiltrated between the PCF region and the silica tube. Epoxy was used to close the two ends of the tube, thereby sealing the PCF inside the tube. The process could create a resistant PCF against strain and bending, thus making the PCF unsuitable for mechanical sensing. However, the device will be more sensitive to the environmental temperature because of the DMSO infiltration. We adopted a new idea to design the modal interferometer. The idea is to decrease the distance of the fusion area between the PCF and SMF tips to zero during fusion. By using this approach, the collapsed air-holes will be more uniform and the two PCF modes can be converted to each other at the fused area.

The voids of the PCF were collapsed in the spliced region, thus allowing the coupling and recombination of PCF core and cladding modes^[17].

Assuming that the interference between the intrinsic light and the recoupled light is expressed as a function of the core mode intensity I_{co} , the cladding mode intensity I_{cl} , and the phase difference φ accumulated during a physical length L ^[18]:

$$I = I_{co} + I_{cl} + 2\sqrt{I_{co}I_{cl}} \cos(2\pi\Delta n/\lambda), \quad (1)$$

where Δn is the difference of the effective refractive index of the core and cladding modes, respectively. The maximum interference signal occurs if $\varphi = 2\pi\Delta nL/\lambda$ between core and cladding modes at $2k\pi$, whereas the minimum interference signal appears when $\varphi = (2k+1)\pi$. The relative phase difference depends on the splicing conditions, mismatch of the modal fields in the PCF-SMF junction, and the surrounding refractive index^[17]. The resonance condition for the interference modes can be given by

$$2\pi\Delta n/\lambda L = m\pi, \quad (2)$$

where $m = 1, 2, 3 \dots$, L is the length of the PCF, and λ is the wavelength of light in vacuum. The free spectral range (FSR) of the interference pattern is given by $\text{FSR} = \lambda^2/\Delta nL$. In our experiment, the excited fundamental core mode during splicing is insensitive to the external environment, whereas the cladding modes are sensitive because of the infiltration of DMSO between the

PCF and the silica tube. Depending on evanescent field theory, the resonance wavelength of the interferometer shifted according to the change in the propagation constant. As the refractive index of DMSO changes, the effective index of the guided modes increases, the Δn in the PCF is modified, and the resonant wavelength shifts. The sensitivity can be described as

$$S = \left(\frac{\partial\lambda}{\partial T}\right) \cdot \left(\frac{\partial T}{\partial\Delta n}\right). \quad (3)$$

An amplified spontaneous emission (ASE) source supplies the necessary wide band input light (C+L band), and an Ando AQ6370 optical spectrum analyzer (OSA) is used as a recorder of the transmission spectra. The device exhibits a sinusoidal interference pattern over a broad wavelength (1525-1610 nm) range. The experimental setup is shown in Fig. 2. A calibrated hotplate was used to heat the PCF. A thermometer with $0.1\text{ }^\circ\text{C}$ graduations was used to record temperature. We tested more than five PCF modal interferometer samples with different lengths to evaluate the temperature dependence of the fiber. The sensitivity of the modal interferometer sensor without DMSO infiltration was only 4-5 pm/ $^\circ\text{C}$.

Due to the high sensitivity of this sensor, we divided the measurements to reflect the ability of this sensor for detecting small temperature variations and to determine the trade-off between the sensing range and the detection limit. Figure 3 shows the transmission spectra of the DMSO-PCF interferometer at 100-180 $^\circ\text{C}$. The interference dips shift when the temperature varied from 100 to 180 $^\circ\text{C}$. This shift is dominantly caused by the evanescent field interaction of the cladding mode with changes in the DMSO refractive index. As a result, the effective refractive indices of core and cladding modes decrease with increasing temperature. Therefore, for every temperature variation, the refractive index of the liquid will be changed and the sensor (PCF section) becomes responsive to the refractive index variation of the liquid. The temperature sensitivity of the sensor reached up to $-0.315\text{ nm}/^\circ\text{C}$. The temperature sensitivity maybe increased by tapering, etching, or side polishing the fiber. The results indicate low interference visibility below 100 $^\circ\text{C}$ for this sensor. This finding is caused by the high refractive index of DMSO (1.4768) compared with the effective refractive index calculated in LMA-8 PCF (1.4452) at 1550 nm. In this case, all cladding modes are lost, and only the core mode can pass the entire PCF. The evanescent waves are restrained with the increasing refractive index of DMSO. DMSO has a high refractive index below 100 $^\circ\text{C}$; thus, the launched beam from ASE will pass through the fiber without coupling with the cladding modes. Therefore, no interference occurs. Consequently, a straight line appears singly on the OSA, indicating the transmission of only the core mode. When the temperature reaches 100 $^\circ\text{C}$, the refractive index of DMSO is lower than that of PCF; therefore, high interference visibility appears on the OSA screen, as shown



Fig. 2. Schematic of the experimental setup.

in Fig. 4(a). Our sensor is adapted to measure the range of temperature variations over 100 °C, which is higher than that of previously reported PCF temperature sensors infiltrated with liquids^[12].

Another feature of the present sensor is seen with the OSA display. Specifically, a straight line appears on the OSA screen, which indicates that the temperature is still below 100 °C. During the experiments, the sensor can be operated at 150 °C, and during day operation, the purity loss is less than 0.1%. The high fringe visibility of the interferometer (10-20 dB) and the high signal-to-noise ratio (SNR; 10-30 dB) show that the interference formation is uniform, which is desired for sensing applications. The linear behavior between the resonant dip wavelengths is shown in Fig. 4(b). The linear fitting of curves can be expressed as $y=1617.630-0.3156x$ and $y=1587.487-0.2836x$. From these equations, the obtained sensitivity reached 0.315 nm/°C at a resonant wavelength of 1617.63 nm and 0.283 nm/°C at a resonant wavelength of 1587.48 nm. The response time of the sensor is higher than that of the conventional PCF temperature sensors because of the high DMSO thermal coefficient of $8.8 \times 10^{-4}/^{\circ}\text{C}$ of the former compared with $10^{-6}/^{\circ}\text{C}$ for fused silica. Thus, multitude sensors with orthogonal geometry for each PCF coupled with DMSO can be produced.

In conclusion, a high-temperature sensitive PCF sensor based on DMSO modal interferometer is designed and built. The DMSO liquid that is adapted for high temperature sensing is sealed between the main PCF and silica tube. In-fiber modal interferometer is used to implement core-cladding modes interference. The cladding modes

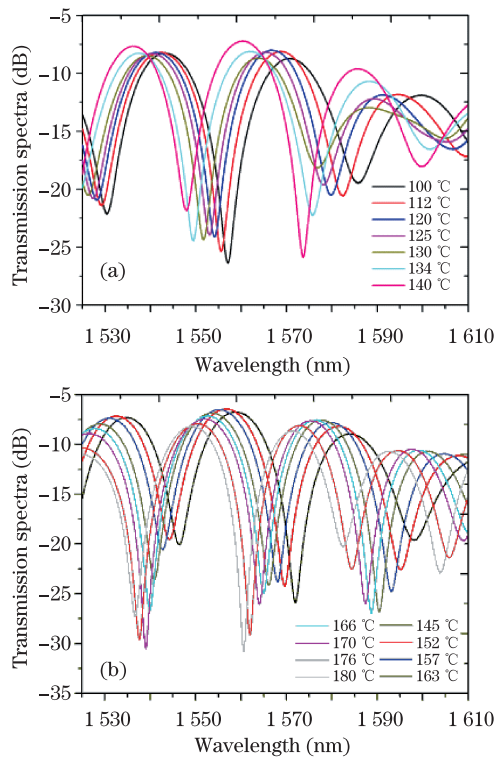


Fig. 3. (Color online) (a) Transmission spectra of DMSO PCF interferometer from 100 to 140 °C in the experiment; (b) transmission spectra of DMSO PCF interferometer from 145 to 180 °C in the experiment.

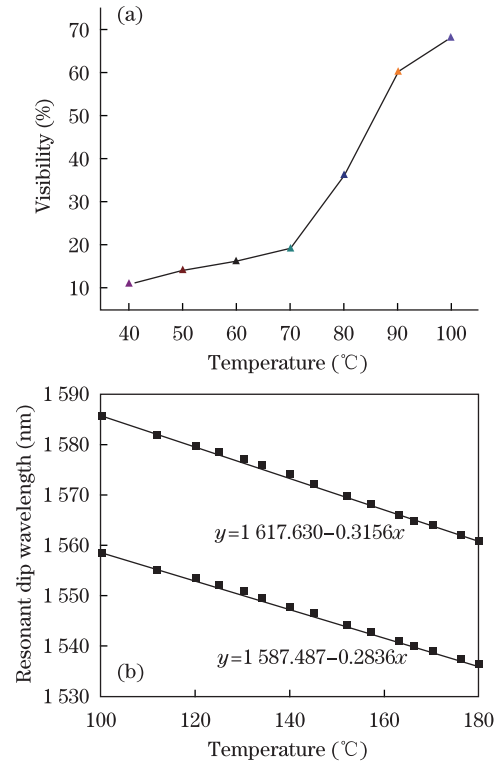


Fig. 4. (Color online)(a) Relationship between fringe visibility and low temperature of DMSO temperature sensor; (b) relationship between temperature and resonant dips from 100 to 180 °C.

interact with the DMSO refractive index depending on the evanescent wave effect. A flat spectrum is observed below 100 °C because of the high refractive index of DMSO and the high scattering effects for cladding modes. Blue shifts in the resonant dip wavelengths are observed with increasing temperature. The effective interaction of PCF cladding modes and DMSO solvent can be achieved by stripping the PCF coating or by decreasing the effective interaction length. A linear relationship between the resonant wavelength and temperature is obtained with temperature sensitivity reaching 0.315 nm/°C. The advantages of the sensor include small size, simplicity, high response time, and high sensitivity. Moreover, the silica tube around the fiber makes the sensor robust. The proposed sensor can be utilized for monitoring small temperature change in highly sensitive devices and for temperature sensing in alarm systems.

One of the authors (A. H. Abdulhadi) would like to thank Professor Yanqing Lu from Nanjing University, China and his group for allowing the author to conduct the experiments at their lab. Abdulhadi extends his gratitude and appreciation to the Iraq Ministry of Higher Education for awarding him a scholarship to carry out a part of this work abroad.

References

1. W. H. Tsai and C. J. Lin, *J. Lightwave Technol.* **19**, 682 (2001).
2. A. Zhang, T. Xia, S. He, and W. Xue, *IEEE Sensor. J.* **10**, 1415 (2010).

3. L. Jiang, J. Yang, S. Wang, B. Li, and M. Wang, *Opt. Lett.* **36**, 3753 (2011)
4. O. Frazao, J. L. Santos, F. M. Araujo, and L. A. Ferreira, *Laser Photon. Rev.* **2**, 449 (2008).
5. Y. Peng, J. Hou, Z. Huang, B. Zhang, and Q. Lu, *Chin. Opt. Lett.* **10**, S10607 (2012).
6. S. Y. Zhang, Q. Zhong, X. S. Qian, X. W. Lin, F. Xu, W. Hu, and Y. Q. Lu, *J. Appl. Phys.* **108**, 023107 (2010).
7. C. C. Chan, X. Y. Dong, Y. P. Wang, P. Zu, W. C. Wong, and W. W. Qian, T. Li, *IEEE Photon. J.* **4**, 114 (2012).
8. J. S. Petrovic, H. Dobb, V. K. Mezentsev, K. Kalli, D. J. Webb, and I. Bennion, *J. Lightwave Technol.* **25**, 1306 (2007).
9. J. Villatoro, V. Finazzi, V. P. Minkovich, V. Pruneri, and G. Badenes, *Appl. Phys. Lett.* **91**, 091109 (2007).
10. S. H. Aref, R. Amezcua-Correa, J. P. Carvalho, O. Frazão, P. Caldas, J. L. Santos, F. M. Araújo, H. Latifi, F. Farahi, L. A. Ferreira, and J. C. Knight, *Opt. Express* **17**, 18669 (2009).
11. S. J. Qiu, Y. Chen, J. L. Kou, F. Xu, and Y. Q. Lu, *Appl. Opt.* **50**, 4328 (2011).
12. S. Qiu, Y. Chen, F. Xu, and Y. Lu, *Opt. Lett.* **37**, 863 (2012).
13. W. Qian, C. L. Zhao, S. He, X. Dong, S. Zhang, Z. Zhang, S. Jin, J. Guo, and H. Wei, *Opt. Lett.* **36**, 1548 (2011).
14. J. Zhang, H. Sun, Q. Rong, Y. Ma, L. Liang, Q. Xu, P. Zhao, Z. Feng, M. Hu, and X. Qiao, *Chin. Opt. Lett.* **10**, 070607 (2012).
15. G. Kvakovszky, A. McKim, and J. Moore, *ECS Trans.* **11**, 227 (2007).
16. J. Villatoro, V. P. Minkovich, V. Pruneri, and G. Badenes, *Opt. Express* **15**, 1491 (2007).
17. W. J. Bock, T. A. Eftimov, P. Mikulic, and J. Chen, *J. Lightwave Technol.* **27**, 3933 (2009).
18. H. P. Gong, C. C. Chan, Y. F. Zhang, W. C. Wong, and X. Y. Dong, *J. Biomed. Opt.* **16**, 017004 (2011).